Pnicogen-bonded cyclic trimers (PH2X)3 with X = F, Cl, OH, NC, CN, CH3, H, and BH2

ARTICLE *in* THE JOURNAL OF PHYSICAL CHEMISTRY A · JUNE 2013

Impact Factor: 2.69 · DOI: 10.1021/jp403651h · Source: PubMed

THE JOURNAL OF PHYSICAL CHEMISTRY A

Article

pubs.acs.org/JPCA

Pnicogen-Bonded Cyclic Trimers $(PH_2X)_3$ with X = F, Cl, OH, NC, CN, CH_3, H, and BH_2

Ibon Alkorta* and José Elguero

Instituto de Química Médica (IQM-CSIC), Juan de la Cierva, 3 28006-Madrid, Spain

Janet E. Del Bene*

Department of Chemistry, Youngstown State University, Youngstown, Ohio 44555, United States

Supporting Information

ABSTRACT: Ab initio MP2/aug'-cc-pVTZ calculations have been carried out to determine the structures and binding energies of cyclic trimers $(PH_2X)_3$ with X = F, Cl, OH, NC, CN, CH_3, H, and BH_2. Except for $[PH_2(CH_3)]_3$, these complexes have C_{3h} symmetry and binding energies between −17 and −63 kJ mol^{-1}. Many-body interaction energy analyses indicate that the two-body terms are dominant, accounting for 97−103% of the total binding energy. Except for the trimer $[PH_2(OH)]_3$, the three-body terms are stabilizing. Charge transfer from the lone pair on one P atom to an antibonding σ^* orbital of the P atom adjacent to the lone pair plays a very significant role in stabilization. The charge-transfer energies correlate linearly with the trimer binding energies. NBO, AIM, and ELF analyses have been used to characterize bonds, lone pairs, and the degree of covalency of the P···P pnicogen bonds. The NMR properties of chemical shielding and $^{31}P-^{31}P$ coupling constants have also been evaluated. Although the ^{31}P chemical shieldings in the five most strongly bound trimers increase relative to the corresponding isolated monomers, there is no correlation between the chemical shieldings and the charges on the P atoms. EOM-CCSD $^{31}P-^{31}P$ spin−spin coupling constants computed for four $(PH_2X)_3$ trimers fit nicely onto a plot of $^{1p}J(P-P)$ versus the P−P distance for $(PH_2X)_2$ dimers. A coupling constant versus distance plot for the four trimers has a second-order trendline which has been used to predict the values of $^{1p}J(P-P)$ for the remaining trimers.

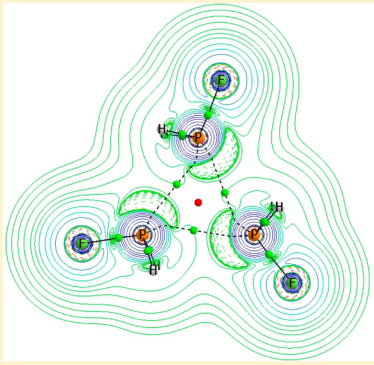

INTRODUCTION

The pnicogen bond is the most recent intermolecular interaction to be incorporated into the list of weak interactions. This bond is a Lewis acid−Lewis base attractive interaction in which a pnicogen atom (N, P, or As) is the Lewis acid. Even though complexes in which a pnicogen atom acts as a Lewis acid have been known for some time,[1−6] it was only subsequent to the landmark paper by Hey-Hawking et al.[7] in 2011 that this interaction came to the forefront of intermolecular interactions. This is evidenced by the number of papers published on the pnicogen bond since then.[8−33]

The electrostatic component of the pnicogen bond has been described in terms of the σ−hole concept proposed by Politzer and Murray.[5] The term σ−hole refers to the electron-deficient outer lobe of a p orbital of an electronegative atom which is involved in bond formation as an electron-pair acceptor. However, Scheiner and his collaborators and much of our earlier work demonstrated that charge transfer from the lone pair of the base to the σ^* P-X orbital of the acid is an extremely important factor in the stabilization of complexes with pnicogen bonds.

Although most of the studies of the pnicogen bond have focused on binary complexes, Adhikari and Scheiner showed that it is possible to form trimers and tetramers consisting of only PH_3 molecules.[17] In the present study, we have investigated a related series of cyclic trimers with the formula $(PH_2X)_3$, illustrated in Scheme 1, with X = F, Cl, OH, NC, CN, CH_3, H, and BH_2. Only local minima which have cyclic equilibrium structures, with each P atom acting as both an electron-pair donor and an electron-pair acceptor, have been included. In this article we report the structures and energies of these trimers, characterize their bonding patterns, and present computed ^{31}P chemical shieldings and $^{31}P-^{31}P$ spin−spin

Scheme 1. Trimers $(PH_2X)_3$

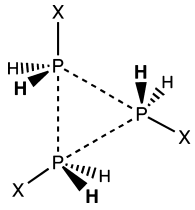

X = F, Cl, OH, NC, CN, CH_3, H, BH_2

Received: April 13, 2013
Revised: May 18, 2013
Published: June 3, 2013

   dx.doi.org/10.1021/jp403651h | J. Phys. Chem. A 2013, 117, 4981−4987

coupling constants. We also compare the trimers $(PH_2X)_3$ with the corresponding dimers $(PH_2X)_2$.

COMPUTATIONAL METHODS

The structures of isolated monomers and complexes were optimized at second-order Møller−Plesset perturbation theory (MP2)[34−37] with the aug'-cc-pVTZ basis set.[38] This basis set is derived from the Dunning aug-cc-pVTZ basis set[39,40] by removing diffuse functions from H atoms. Frequencies were computed to establish that the optimized structures correspond to equilibrium structures on their potential surfaces. All optimization and frequency calculations were performed using the Gaussian 09 program.[41]

The many body interaction energy (MBIE) partitioning method[42,43] has been used to examine the binding energies ΔE of the trimers. For this study, ΔE is defined as the difference between the energy of the trimer at its equilibrium geometry and the sum of the energies of the corresponding isolated monomers. ΔE can be decomposed into a series of terms which depend on one-, two-, and three-body interactions.

$$\Delta E = E(123) - \sum_{i=1}^{3} E_m(i)$$

$$= \sum_{i=1}^{3} [E(i) - E_m(i)] + \sum_{i=1}^{2} \sum_{j>i}^{3} \Delta^2 E(ij) + \Delta^3 E(123)$$

$$E_R(i) = E(i) - E_m(i)$$

$$\Delta^2 E(ij) = E(ij) - [E(i) + E(j)]$$

$$\Delta^3 E(123) = E(123) - [E(1) + E(2) + E(3)] - [\Delta^2 E(12) + \Delta^2 E(13) + \Delta^2 E(23)]$$

$E_m(i)$ is the energy of an isolated, optimized monomer. The terms $E(i)$, $E(ij)$, and $E(123)$ are the energies of the monomers, dimers, and trimer, computed at their geometries in the complex. $E_R(i)$ is the monomer relaxation energy, $\Delta^2 E(ij)$ is a two-body interaction energy, and $\Delta^3 E(123)$ is the three-body interaction energy.

The electron densities of the pnicogen trimers have been analyzed with the atoms in molecules (AIM) methodology[44−47] and the electron localization function (ELF)[48] using the AIMAll[49] and Topmod[50] programs. The topological analysis of the electron density produces the molecular graph of each complex. This graph identifies the location of electron density features of interest. These include the electron density (ρ) maxima associated with the various nuclei, saddle points which corresponds to bond critical points (BCPs), and ring critical points which indicate a minimum electron density within a ring. The zero gradient line which connects a BCP with two nuclei is the bond path. The electron density at the BCP (ρ_{BCP}), the Laplacian of the electron density at the BCP ($\nabla^2\rho_{BCP}$), and the total energy density (H_{BCP}) are additional useful quantities for characterizing interactions.[51] The ELF function illustrates those regions of space at which the electron density is high. Using all of these measures, bonds and lone pairs can be easily identified, and bond types can be characterized.

The natural bond orbital (NBO) method[52] has been used to obtain atomic charges and to analyze the stabilizing charge-transfer interactions in the trimers. The NBO-5 program[53] within the Gamess program[54] has been used for the NBO calculations. The molecular electrostatic potentials (MEPs) of the isolated monomers have been calculated with the Gaussian 09 program. These have been represented on the 0.001 au electron density isosurface using the WFA program.[55]

Absolute chemical shieldings have been calculated for all trimers at MP2/aug'-cc-pVTZ using the GIAO approximation.[56] Coupling constants were evaluated for $(PH_3)_3$, $(PH_2F)_3$, $[PH_2(OH)]_3$, and $[PH_2(CH_3)]_3$ using the equation-of-motion coupled cluster singles and doubles (EOM-CCSD) method in the CI (configuration interaction)-like approximation,[57,58] with all electrons correlated. For these calculations, the Ahlrichs[59] qzp basis set was placed on ^{13}C, ^{15}N, ^{17}O, and ^{19}F and the qz2p basis set on ^{31}P and ^{35}Cl. The Dunning cc-pVDZ basis set was placed on all H atoms. Only $^{1p}J(P-P)$ coupling constants are reported in this paper. The EOM-CCSD calculations were performed using ACES II[60] on the IBM Cluster 1350 (Glenn) at the Ohio Supercomputer Center.

RESULTS AND DISCUSSION

Structures and Energies. The P−P distances, A−P···P angles, and the binding energies ΔE of the trimers $(PH_2X)_3$ are reported in Table 1. Corresponding data for $(PH_2X)_2$ dimers are also reported for comparative purposes. The cyclic trimers have equilibrium structures of C_{3h} symmetry, except for $[PH_2(CH_3)]_3$, which at this geometry has two small degenerate imaginary frequencies of −18 cm^{-1} corresponding to a rocking motion of the H atoms at both ends of each molecule. The equilibrium $[PH_2(CH_3)]_3$ structure has C_1 symmetry but is only 0.25 kJ mol^{-1} more stable than the C_{3h} structure. The intermolecular P−P distances in the trimers range from 2.97 Å in $(PH_2F)_3$ to 3.93 Å in $[PH_2(BH_2)]_3$. The A−P···P angles are between 159 and 171°, where A is the atom of X directly bonded to P. An alignment which approaches linearity has been previously associated with the stability of pnicogen dimers and binary complexes.[20,21] The trimer binding energies range from −17.1 kJ/mol for $(PH_3)_3$ to −62.9 kJ mol^{-1} for $(PH_2F)_3$. A second order polynomial correlates the interaction energies and the intermolecular P−P distances, as illustrated in Figure 1.

Table 1. Binding Energies (ΔE, kJ mol^{-1}), Intermolecular P−P Distances (R, Å) and A−P···P Angles (<, °) for $(PH_2X)_3$ and $(PH_2X)_2$

	$(PH_2X)_3$			$(PH_2X)_2$[a]		
monomer	ΔE	R	<	ΔE	R	<
PH_2F	−62.90	2.974	171	−33.97	2.471	163
PH_2Cl	−49.55	3.144	171	−22.10	2.771	167
$PH_2(OH)$	−43.87	3.229	168	−20.55	2.851	169
$PH_2(NC)$	−37.35	3.272	170	−13.76	3.040	168
$PH_2(CCH)$	−30.29	3.549	166	−12.23	3.353	174
$PH_2(CN)$	−23.68	3.541	168	−8.37	3.375	171
$PH_2(CH_3)$[b]	−18.79	3.738	161	−8.88	3.481	178
PH_3	−17.05	3.809	159	−7.08	3.589	179
$PH_2(BH_2)$	−18.13	3.926	164	−7.04	3.744	174

[a]Data from ref 20. [b]C_{3h} structure.

The P−P distances in trimers $(PH_2X)_3$ are longer than those in the corresponding dimers $(PH_2X)_2$. The order of increasing P−P distance is the same in the dimers and trimers, except for a reversal of $[PH_2(CCH)]_3$ and $[PH_2(CN)]_3$, in which case the distance in the latter is shorter by 0.009 Å. The differences in intermolecular P−P distances vary between 0.17 Å for X = CN, to 0.50 Å for X = F. In addition, the total binding energy and

dx.doi.org/10.1021/jp403651h | J. Phys. Chem. A 2013, 117, 4981−4987

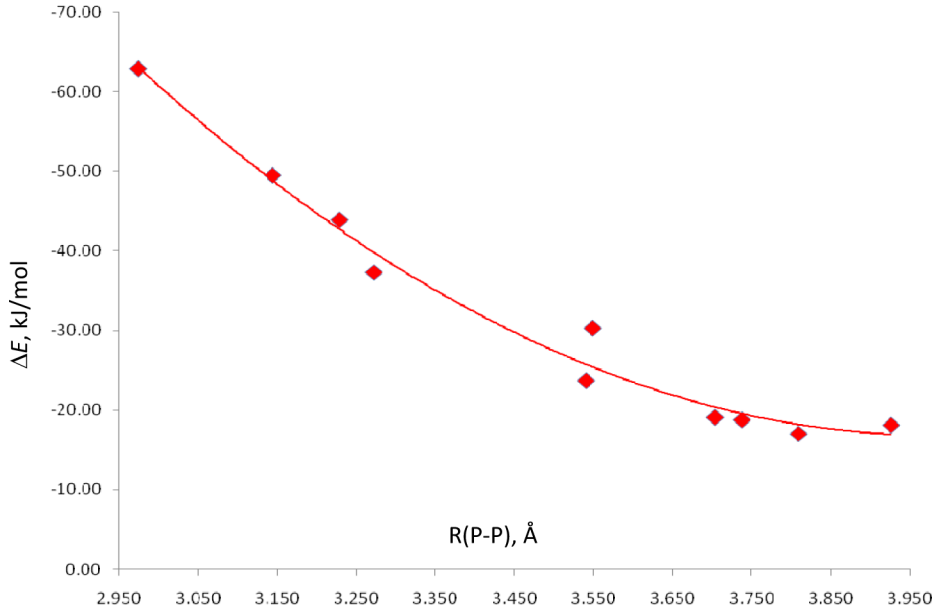

Figure 1. Trimer binding energy (ΔE) versus the P−P distance [R(P−P)] for trimers $(PH_2X)_3$. The correlation coefficient R^2 = 0.981.

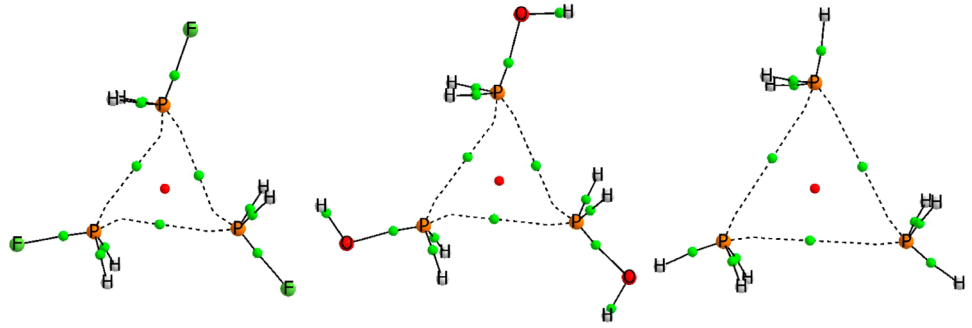

Figure 2. Molecular graphs of trimers $(PH_2F)_3$, $[PH_2(OH)]_3$, and $(PH_3)_3$. Green and red dots indicate the positions of bond and ring critical points, respectively. The dashed lines connecting the P atoms and the BCP are the bond paths.

the energy per P···P bond is always greater for the trimer compared to the corresponding dimer. Linear correlations exist between the P−P distances in the trimers and corresponding dimers, and between corresponding binding energies, as given by eqs 1 and 2.

$$[R(\text{P-P}), (PH_2X)_3] = 0.76[R(\text{P-P}), (PH_2X)_2] + 1.04 \quad R^2 = 0.97 \tag{1}$$

$$\Delta E(PH_2X)_3 = 1.74[(PH_2X)_2] - 7.7 \quad R^2 = 0.95 \tag{2}$$

The results of the many body interaction energy analyses of the trimers are reported in Table 2. These data indicate that the monomer relaxation energy, $E_R(1)$, is relatively small at no more than 0.90 kJ/mol per monomer. As anticipated, the most important energy component arises from the two-body interactions $\Sigma\Delta^2E$ which account for 97 to 103% of the total binding energy. An excellent linear correlation is obtained between $\Sigma\Delta^2E$ and ΔE, with a correlation coefficient R^2 = 0.999. With one exception, the three-body term, Δ^3E, is stabilizing and ranges from −0.12 kJ/mol for $[PH_2(BH_2)]_3$ to −2.38 kJ/mol for $[PH_2(CN)]_3$. The sole exception is found for the $[PH_2(OH)]_3$ complex which has a destabilizing three-body term of +0.45 kJ/mol.

Table 2. MBIE Components of the Interaction Energies (kJ/mol) of Trimers with C_{3h} Symmetry

	$E_R(1)^a$	ΣE_R	$\Delta^2E(1,2)^a$	$\Sigma\Delta^2E$	$\Delta^3E(1,2,3)$
$(PH_2F)_3$	0.90	2.70	−21.48	−64.44	−1.16
$(PH_2Cl)_3$	0.50	1.50	−16.58	−49.74	−1.29
$[PH_2(OH)]_3$	0.24	0.72	−15.01	−45.03	0.45
$[PH_2(NC)]_3$	0.40	1.20	−12.06	−36.18	−2.38
$[PH_2(CCH)]_3$	0.12	0.36	−10.12	−30.36	−0.29
$[PH_2(CN)]_3$	0.19	0.57	−7.64	−22.92	−1.32
$[PH_2(CH_3)]_3$	0.05	0.15	−6.13	−18.39	−0.53
$(PH_3)_3$	0.05	0.15	−5.61	−16.83	−0.36
$[PH_2(BH_2)]_3$	0.08	0.24	−6.08	−18.24	−0.12

[a]For these trimers, $E_R(1) = E_R(2) = E_R(3)$ and $\Delta^2E(1,2) = \Delta^2E(1,3) = \Delta^2E(2,3)$.

The second-order NBO analysis provides an evaluation of the stabilization energy due to charge transfer from the lone pair of one P atom to the σ^* P−A orbital of the other P atom which is adjacent to the lone pair, with A the atom of X directly bonded to P. The stabilization energies due to charge transfer are reported in Table 3. These charge-transfer energies follow the same ordering as the trimer binding energies, except for $[(PH_2(OH)]_3$. In this complex, there is a secondary back-donation that is not present in the other complexes, from the

dx.doi.org/10.1021/jp403651h | J. Phys. Chem. A 2013, 117, 4981−4987

Table 3. P(lp) → σ*P−A Charge Transfer Energies and Changes in P−A Bond Lengths [δR(P−P)] in Trimers $(PH_2X)_3$

trimers	P(lp) → σ*P−A,[a] kJ mol^{-1}	δR(P−A) (Å)
$(PH_2F)_3$	50.5	0.006
$(PH_2Cl)_3$	30.6	0.009
$[PH_2(OH)]_3$	26.4	0.004
$[PH_2(NC)]_3$	26.9	0.001
$[PH_2(CCH)]_3$	11.0	0.003
$[PH_2(CN)]_3$	11.8	0.001
$[PH_2(CH_3)]_3$	5.6	0.002
$(PH_3)_3$	5.3	0.002
$[PH_2(BH_2)]_3$	3.0	−0.003

[a]A is the atom of X which is directly bonded to P.

P(lp) → σ* P−O orbital, with a stabilization energy of 4.1 kJ mol^{-1}. A linear correlation exists between the binding energies of the trimers and the charge-transfer energies, with a correlation coefficient R^2 = 0.958. In all trimers, the increased population of the σ* P−A orbital leads to a lengthening of the P−A bond relative to the monomer, except for $[PH_2(BH_2)]_3$. The changes in P−A bond lengths are also reported in Table 3.

Bonding Characteristics. The ELF isosurface of each trimer shows the location of the P lone pairs, as illustrated in Figure 3a for $(PH_2F)_3$. This information, combined with the

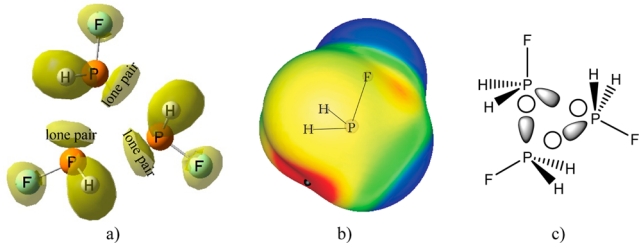

Figure 3. (a) ELF 0.75e isosurface of $(PH_2F)_3$, illustrating the P lone pair basins. (b) The MEP on the 0.001 au electron density isosurface of the isolated PH_2F molecule. The location of the σ-hole maxima (0.060 au) is indicated with a black dot. Color code scale (au): red > 0.03 > yellow > 0.015 > green > 0.0 > blue. (c) Schematic representation of the lone pairs and σ-holes, represented as empty circles, of the $(PH_2F)_3$ trimer.

MEP of the isolated monomer in Figure 3b, provides a clear picture of the electrostatic interaction between the lone pairs and the σ-holes shown schematically in Figure 3c, in agreement with previous reports.[61] The AIM analyses of the trimers show the three intermolecular bond critical points (BCPs) that connect the phosphorus atoms, and a ring critical point in Figure 2. The electron densities at P···P BCPs range from 0.006 to 0.026 au and correlate exponentially with the P−P distance with an R^2 value of 0.9996, in agreement with previous reports that have shown similar relationships for other weak interactions.[62−71] The P···P bond paths show a significant curvature, especially in the more strongly bound complexes. The bond path is longer than the intermolecular P−P distance by as much as 0.15 Å in $(PH_2F)_3$ but by only 0.015 Å in $[PH_2(BH_2)]_3$. The simultaneous representation of the Laplacian and the bond path in Figure 4 indicates that the bond path leads from one P atom where the concentration of lone pair electron density is high and the Laplacian is negative, to the

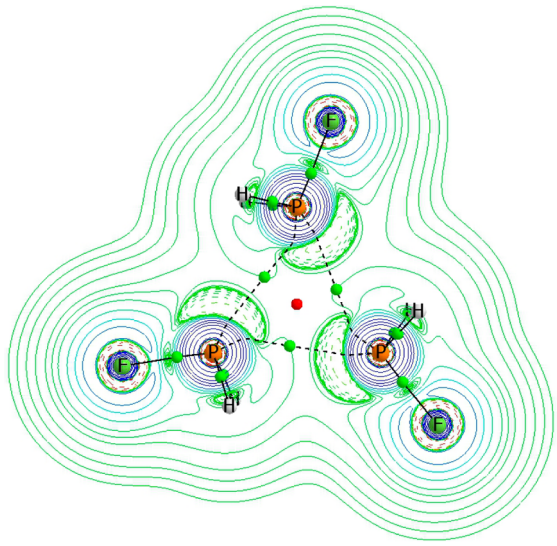

Figure 4. Laplacian contours in the symmetry plane and molecular graph of $(PH_2F)_3$. Negative values of the Laplacian are indicated with dashed lines.

σ-hole of the adjacent P atom, avoiding the region of electron concentration on the latter P.

The signs of the Laplacian ($\nabla^2\rho_{BCP}$) and the total energy density (H_{BCP}) at the BCPs can be used to characterize the nature of the intermolecular interactions in these trimers. $\nabla^2\rho_{BCP}$ is always positive, while H_{BCP} is positive for the more weakly bound trimers but negative for the five most strongly bound trimers. Thus, some partial covalent character can be ascribed to the pnicogen bonds in the latter.[51]

NMR Properties. *Absolute Chemical Shieldings.* The ^{31}P absolute chemical shieldings in monomers, dimers, and trimers, the charges on P in the trimers, and changes in these quantities are reported in Table 4. The chemical shieldings in the monomers are determined by the substituents X. Except for X = F, the changes in these shieldings in the dimers and trimers relative to the corresponding monomers are relatively small. The shieldings increase relative to the monomers in the four most strongly bound dimers and trimers with X = F, Cl, OH, and NC, and decrease in the remaining dimers and trimers. However, there is no correlation between the charge on P and the chemical shielding, or the change in the charge on P and the change in the chemical shielding in the trimers relative to the corresponding monomers.

Coupling Constants. Because of the computational cost associated with EOM-CCSD calculations, coupling constants have been computed for only four trimers, two of the most strongly bound ones {$(PH_2F)_3$ and $[PH_2(OH)]_3$}, and two of the more weakly bound trimers {$[PH_2(CH_3)]_3$ and $(PH_3)_3$}. In ref 20 we demonstrated that the FC term is an excellent approximation to ^{1p}J(P−P) in dimers $(PH_2X)_2$, so only the FC terms have been computed for three trimers and total ^{1p}J(P−P) for $(PH_3)_3$. The values of these coupling constants are reported in Table 5. Figure 5 provides a plot of the FC terms for the trimers and ^{1p}J(P−P) for the corresponding dimers $(PH_2X)_2$ against the intermolecular P−P distance. The trendline including all points has a correlation coefficient of 0.967, indicating that the trimer points correlate very nicely with the dimer points. However, the range of ^{1p}J(P−P) for the dimers is very large (1000 Hz), and the curvature of the trendline is certainly influenced by the value of ^{1p}J(P−P) for $(PH_2F)_2$ at its

dx.doi.org/10.1021/jp403651h | J. Phys. Chem. A 2013, 117, 4981−4987

Table 4. Absolute Chemical Shieldings (σ, ppm) for Monomers, Dimers, and Trimers, Charges (e) on P in Trimers $(PH_2X)_3$, and Changes (Δ) in These Quantities

trimer	$\sigma(n = 1)$	$\sigma(n = 2)$	$\sigma(n = 3)$	$\Delta\sigma(2-1)$	$\Delta\sigma(3-1)$	charge	Δcharge(3−1)
$(PH_2F)_n$	272.76	354.02	348.33	81.27	75.58	0.678	−0.057
$(PH_2Cl)_n$	420.43	443.91	442.24	23.48	21.81	0.307	−0.037
$[PH_2(OH)]_n$	340.25	358.30	360.68	18.05	20.44	0.608	−0.013
$[PH_2(NC)]_n$	454.50	459.72	463.79	5.22	9.29	0.527	−0.046
$[PH_2(CCH)]_n$	566.87	560.68	556.36	−6.19	−10.51	0.323	−0.025
$[PH_2(CN)]_n$	577.71	572.25	568.32	−5.46	−9.39	0.290	−0.038
$[PH_2(CH_3)]_n$	548.57	540.14	533.67	−8.43	−14.90	0.287	0.001
$(PH_3)_n$	633.25	626.31	621.06	−6.95	−12.19	0.005	−0.004
$[PH_2(BH_2)]_n$	522.43	512.43	501.04	−10.00	−21.39	0.010	−0.008

Table 5. Spin−Spin Coupling Constants [^{1p}J(P−P), Hz] Approximated as FC Terms for Selected Trimers

trimer	computed FC terms	estimated $^{1p}J(P-P)^a$
$(PH_2F)_3$	502.0	503
$(PH_2Cl)_3$		384
$[PH_2(OH)]_3$	331.6	332
$[PH_2(NC)]_3$		306
$[PH_2(CCH)]_3$		172
$[PH_2(CN)]_3$		175
$[PH_2CH_3)]_3$	103.6[b]	106
$(PH_3)_3$	86.8[c]	86
$[PH_2(BH_2)]_3$		61

[a]Estimated from the equation of the trendline for the four trimers. [b]C_{3h} structure. [c]Total ^{1p}J(P−P) is 86.9 Hz.

short P−P distance. The correlation coefficient of the trendline for the four trimers is 1.000, and this trendline has a reduced curvature. The equation for this trendline has been used to obtain estimates of ^{1p}J(P−P) for the trimers, which are also reported in Table 5.

CONCLUSIONS

Ab initio calculations have been carried out on cyclic pnicogen-bonded trimers $(PH_2X)_3$, with X = F, Cl, OH, NC, CN, CH_3, H, and BH_2, to determine their structures, binding energies, bonding properties, ^{31}P chemical shieldings, and $^{31}P-^{31}P$ spin−spin coupling constants. These calculations support the following statements.

(1) The equilibrium trimer structures have C_{3h} symmetry except for $[PH_2(CH_3)]_3$ which has only C_1 symmetry. However, the equilibrium trimer is only 0.25 kJ mol^{-1} more stable than the C_{3h} structure. The P−P distances in the trimers range from 2.97 to 3.93 Å.

(2) The trimer binding energies vary from −17 to −63 kJ mol^{-1}. The many-body interaction energy analyses show that the two-body terms account for 97 to 103% of the total binding energies. Except for the trimer $[PH_2(OH)]_3$, the three-body terms are stabilizing. While both electrostatic and polarization components stabilize these trimers, charge transfer from the lone pair of one P atom to the σ^* P−A orbital of the P atom adjacent to the lone pair plays a very significant role in stabilization. The charge-transfer energies correlate linearly with the binding energies of the trimers.

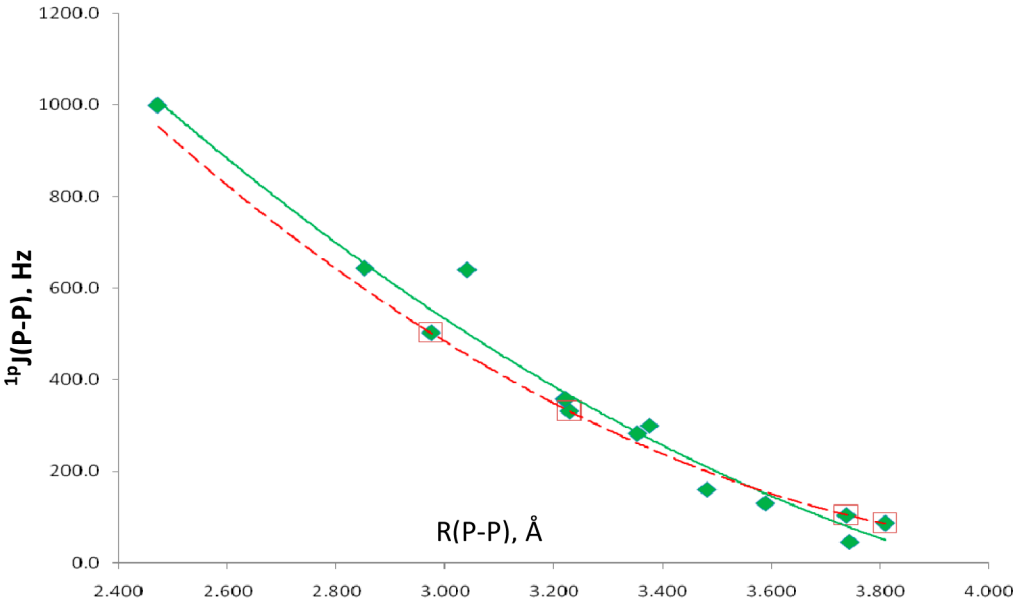

Figure 5. ^{1p}J(P−P) total coupling constants versus the P−P distance for dimers $(PH_2X)_2$ and the FC terms for four trimers $(PH_2X)_3$ versus the P−P distance. The four points belonging to the trimers $(PH_3)_3$, $(PH_2F)_3$, $(PH_2OH)_3$, and $(PH_2CH_3)_3$ are enclosed in red boxes. The solid trendline refers to all complexes, and the dashed trendline refers only to the trimers.

dx.doi.org/10.1021/jp403651h | J. Phys. Chem. A 2013, 117, 4981−4987

(3) AIM, NBO, and ELF analyses describe bonds, lone pairs, and σ-holes in these complexes and indicate that the five most strongly bound trimers have pnicogen bonds with some covalent character.

(4) The ^{31}P chemical shieldings in the five most strongly bound trimers increase relative to the corresponding isolated monomers. However, there is no correlation between charges on P atoms and chemical shieldings.

(5) The ^{31}P–^{31}P spin–spin coupling constants computed for four $(PH_2X)_3$ trimers fit nicely onto the plot of ^{1p}J(P–P) versus the P–P distance for the $(PH_2X)_2$ dimers. The coupling constant versus distance plot for the four trimers has a second-order trendline which has been used to predict values of ^{1p}J(P–P) for the remaining trimers.

■ ASSOCIATED CONTENT

Supporting Information

MP2/aug'-cc-pVTZ total energies and optimized geometries for trimers $(PH_2X)_3$; full references 41, 54, and 60. This material is available free of charge via the Internet at http://pubs.acs.org.

■ AUTHOR INFORMATION

Corresponding Author

*E-mail: ibon@iqm.csic.es; jedelbene@ysu.edu.

Notes

The authors declare no competing financial interest.

■ ACKNOWLEDGMENTS

This work was carried out with financial support from the Ministerio de Economía y Competitividad (Project No. CTQ2012-35513-C02-02) and Comunidad Autónoma de Madrid (Project MADRISOLAR2, ref S2009/PPQ1533). Thanks are also given to the Ohio Supercomputer Center for its continued support and to the CTI (CSIC) for a grant of computer time.

■ REFERENCES

(1) Widhalm, M.; Kratky, C. Synthesis and X-ray Structure of Binaphthyl-Based Macrocyclic Diphosphanes and Their Ni(II) and Pd(II) Complexes. *Chem. Ber.* **1992**, *125*, 679–689.

(2) Drago, R. S.; Wong, N.; Ferris, D. C. The E, C, T Interpretation of Bond Dissociation Energies and Anion-Neutral Molecule Interactions. *J. Am. Chem. Soc.* **1991**, *113*, 1970–1977.

(3) Carré, F.; Chuit, C.; Corriu, R. J. P.; Mongorte, P.; Nayyar, N. K.; Reyé, C. Intramolecular Coordination at Phosphorus: Donor-Acceptor Interaction in Three- and Four-Coordinated Phosphorus Compounds. *J. Organomet. Chem.* **1995**, *499*, 147–154.

(4) Klinkhammer, K. W.; Pyykko, P. Ab Initio Interpretation of the Closed-Shell Intermolecular E···E Attraction in Dipnicogen $(H_2E\text{-}EH_2)_2$ and Dichalcogen $(HE\text{-}EH)_2$ Hydride Model Dimers. *Inorg. Chem.* **1995**, *34*, 4134–4138.

(5) Murray, J. S.; Lane, P.; Politzer, P. A Predicted New Type of Directional Noncovalent Interaction. *Int. J. Quantum Chem.* **2007**, *107*, 2286–2292.

(6) Mohajeri, A.; Pakirai, A. H.; Bagheri, N. Theoretical Studies on the Nature of Bonding in σ-Hole Complexes. *Chem. Phys. Lett.* **2009**, *467*, 393–397.

(7) Zahn, S.; Frank, R.; Hey-Hawkins, E.; Kirchner, B. Pnicogen Bonds: A New Molecular Linker? *Chem.—Eur. J.* **2011**, *17*, 6034–6038.

(8) Solimannejad, M.; Gharabaghi, M.; Scheiner, S. SH···N and SH···P Blue-Shifting H-Bonds and N···P Interactions in Complexes Pairing HSN with Amines and Phosphines. *J. Chem. Phys.* **2011**, *134* (024312), 1–6.

(9) Scheiner, S. A New Noncovalent Force: Comparison of P···N Interaction with Hydrogen and Halogen Bonds. *J. Chem. Phys.* **2011**, *134* (094315), 1–9.

(10) Scheiner, S. Effects of Substituents upon the P···N Noncovalent Interaction: The Limits of Its Strength. *J. Phys. Chem. A* **2011**, *115*, 11202–11209.

(11) Politzer, P.; Murray, J. Halogen Bonding and Beyond: Factors Influencing the Nature of CN–R and SiN–R Complexes with F–Cl and Cl_2. *Theor. Chem. Acc.* **2012**, *131* (1114), 1–10.

(12) Adhikari, U.; Scheiner, S. Substituent Effects on Cl···N, S···N, and P···N Noncovalent Bonds. *J. Phys. Chem. A* **2012**, *116*, 3487–3497.

(13) Adhikari, U.; Scheiner, S. Sensitivity of Pnicogen, Chalcogen, Halogen and H-Bonds to Angular Distortions. *Chem. Phys. Lett.* **2012**, *532*, 31–35.

(14) Scheiner, S. Can Two Trivalent N Atoms Engage in a Direct N···N Noncovalent Interaction? *Chem. Phys. Lett.* **2011**, *514*, 32–35.

(15) Scheiner, S. Effects of Multiple Substitution upon The P···N Noncovalent Interaction. *Chem. Phys.* **2011**, *387*, 79–84.

(16) Scheiner, S. On the Properties of X···N Noncovalent Interactions for First-, Second-, and Third-Row X Atoms. *J. Chem. Phys.* **2011**, *134* (164313), 1–9.

(17) Adhikari, U.; Scheiner, S. Comparison of P···D (D = P, N) with other Noncovalent Bonds in Molecular Aggregates. *J. Chem. Phys.* **2011**, *135* (184306), 1–10.

(18) Scheiner, S.; Adhikari, U. Abilities of Different Electron Donors (D) to Engage in a P···D Noncovalent Interaction. *J. Phys. Chem. A* **2011**, *115*, 11101–11110.

(19) Scheiner, S. Weak H-Bonds. Comparisons of CHO to NHO in Proteins and PHN to Direct PN Interactions. *Phys. Chem. Chem. Phys.* **2011**, *13*, 13860–13872.

(20) Del Bene, J. E.; Alkorta, I.; Sánchez-Sanz, G.; Elguero, J. ^{31}P–^{31}P Spin–Spin Coupling Constants for Pnicogen Homodimers. *Chem. Phys. Lett.* **2011**, *512*, 184–187.

(21) Del Bene, J. E.; Alkorta, I.; Sánchez-Sanz, G.; Elguero, J. Structures, Energies, Bonding, and NMR Properties of Pnicogen Complexes $H_2XP{:}NXH_2$ (X = H, CH_3, NH_2, OH, F, Cl). *J. Phys. Chem. A* **2011**, *115*, 13724–13731.

(22) Adhikari, U.; Scheiner, S. Effects of Carbon Chain Substituents on the P···N Noncovalent Bond. *Chem. Phys. Lett.* **2012**, *536*, 30–33.

(23) Li, Q.-Z.; Li, R.; Liu, X.-F.; Li, W.-Z.; Cheng, J.-B. Pnicogen–Hydride Interaction between FH_2X (X = P and As) and HM (M = ZnH, BeH, MgH, Li, and Na). *J. Phys. Chem. A* **2012**, *116*, 2547–2553.

(24) Li, Q.-Z.; Li, R.; Liu, X.-F.; Li, W.-Z.; Cheng, J.-B. Concerted Interaction between Pnicogen and Halogen Bonds in $XCl\text{-}FH_2P\text{-}NH_3$ (X = F, OH, CN, NC, and FCC). *ChemPhysChem* **2012**, *13*, 1205–1212.

(25) Del Bene, J. E.; Alkorta, I.; Sánchez-Sanz, G.; Elguero, J. Structures, Binding Energies, and Spin–Spin Coupling Constants of Geometric Isomers of Pnicogen Homodimers $(PHFX)_2$, X = F, Cl, CN, CH_3, NC. *J. Phys. Chem. A* **2012**, *116*, 3056–3060.

(26) Del Bene, J. E.; Alkorta, I.; Sánchez-Sanz, G.; Elguero, J. Homo- and Heterochiral Dimers $(PHFX)_2$, X = Cl, CN, CH_3, NC: To What Extent Do They Differ? *Chem. Phys. Lett.* **2012**, *538*, 14–18.

(27) Alkorta, I.; Sánchez-Sanz, G.; Elguero, J.; Del Bene, J. E. Influence of Hydrogen Bonds on the P···P Pnicogen Bond. *J. Chem. Theor. Comp.* **2012**, *8*, 2320–2327.

(28) An, X.-L.; Li, R.; Li, Q.-Z.; Liu, X.-F.; Li, W.-Z.; Cheng, J.-B. Substitution, Cooperative, and Solvent Effects on π Pnicogen Bonds in the FH_2P and FH_2As Complexes. *J. Mol. Model.* **2012**, *18*, 4325–4332.

(29) Bauzá, A.; Quiñonero, D.; Deyà, P. M.; Frontera, A. Pnicogen-π Complexes: Theoretical Study and Biological Implications. *Phys. Chem. Chem. Phys.* **2012**, *14*, 14061–14066.

(30) Alkorta, I.; Sánchez–Sanz, G.; Elguero, J.; Del Bene, J. E. Exploring $(NH_2F)_2$, $H_2FP{:}NFH_2$, and $(PH_2F)_2$ Potential Surfaces: Hydrogen Bonds or Pnicogen Bonds? *J. Phys. Chem. A* **2013**, *117*, 183–191.

(31) Sánchez−Sanz, G.; Alkorta, I.; Elguero, J. Intramolecular Pnicogen Interactions in PHF−$(CH_2)_n$−PHF (n = 2−6) Systems. *ChemPhysChem* **2013**, *14*, 1656−1665.
(32) Del Bene, J. E.; Alkorta, I.; Sánchez-Sanz, G.; Elguero, J. Phosphorus as a Simultaneous Electron-Pair Acceptor in Intermolecular P···N Pnicogen Bonds and Electron-Pair Donor to Lewis Acids. *J. Phys. Chem. A* **2013**, *117*, 3133−3141.
(33) Grabowski, S. J.; Alkorta, I.; Elguero, J. Complexes between Dihydrogen and Amine, Phosphine, and Arsine Derivatives. Hydrogen Bond versus Pnictogen Interaction. *J. Phys. Chem. A* **2013**, *117*, 3243−3251.
(34) Pople, J. A.; Binkley, J. S.; Seeger, R. Theoretical Models Incorporating Electron Correlation. *Int. J. Quantum Chem., Quantum Chem. Symp.* **1976**, *10*, 1−19.
(35) Krishnan, R.; Pople, J. A. Approximate Fourth-Order Perturbation Theory of the Electron Correlation Energy. *Int. J. Quantum Chem.* **1978**, *14*, 91−100.
(36) Bartlett, R. J.; Silver, D. M. Many−Body Perturbation Theory Applied to Electron Pair Correlation Energies. I. Closed-Shell First−Row Diatomic Hydrides. *J. Chem. Phys.* **1975**, *62*, 3258−3268.
(37) Bartlett, R. J.; Purvis, G. D. Many−Body Perturbation Theory, Coupled-Pair Many-Electron Theory, and the Importance of Quadruple Excitations for the Correlation Problem. *Int. J. Quantum Chem.* **1978**, *14*, 561−581.
(38) Del Bene, J. E. Proton Affinities of Ammonia, Water, and Hydrogen Fluoride and their Anions: A Quest for the Basis-Set Limit Using the Dunning Augmented Correlation-Consistent Basis Sets. *J. Phys. Chem.* **1993**, *97*, 107−110.
(39) Dunning, T. H. Gaussian Basis Sets for Use in Correlated Molecular Calculations. I. The Atoms Boron through Neon and Hydrogen. *J. Chem. Phys.* **1989**, *90*, 1007−1023.
(40) Woon, D. E.; Dunning, T. H. Gaussian Basis Sets for use in Correlated Molecular Calculations. V. Core−Valence Basis Sets for Boron through Neon. *J. Chem. Phys.* **1995**, *103*, 4572−4585.
(41) Frisch, M. J.; et al. *Gaussian 09*, revision A.01; Gaussian, Inc.: Wallingford CT, 2009.
(42) Hankins, D.; Moskowitz, J. W.; Stillinger, F. H. Water Molecule Interactions. *J. Chem. Phys.* **1970**, *53*, 4544−4554.
(43) Xantheas, S. Ab Initio Studies of Cyclic Water Clusters $(H_2O)_N$, N = 1−6. II. Analysis of Many−Body Interactions. *J. Chem. Phys.* **1994**, *100*, 7523−7534.
(44) Bader, R. F. W. A Quantum Theory of Molecular Structure and Its Applications. *Chem. Rev.* **1991**, *91*, 893−928.
(45) Bader, R. F. W. *Atoms in Molecules, A Quantum Theory*; Oxford University Press: Oxford, 1990.
(46) Popelier, P. L. A. *Atoms In Molecules. An introduction*; Prentice Hall: Harlow, England, 2000.
(47) Matta, C. F.; Boyd, R. J. *The Quantum Theory of Atoms in Molecules: From Solid State to DNA and Drug Design*; Wiley-VCH: Weinheim, Germany, 2007.
(48) Silvi, B.; Savin, A. Classification of Chemical Bonds Based on Topological Analysis of Electron Localization Functions. *Nature* **1994**, *371*, 683−686.
(49) AIMAll (Version 11.08.23), Todd, A., Keith, T. K., Eds.; Gristmill Software; Overland Park KS, 2011; aim.tkgristmill.com.
(50) Noury, S.; Krokidis, X.; Fuster, F.; Silvi, B. *TopMod Package*, 1997.
(51) Rozas, I.; Alkorta, I.; Elguero, J. Behavior of Ylides Containing N, O, and C Atoms as Hydrogen Bond Acceptors. *J. Am. Chem. Soc.* **2000**, *122*, 11154−11161.
(52) Reed, A. E.; Curtiss, L. A.; Weinhold, F. Intermolecular Interactions from a Natural Bond Orbital, Donor-Acceptor Viewpoint. *Chem. Rev.* **1988**, *88*, 899−926.
(53) Glendening, E. D.; Badenhoop, J. K.; Reed, A. E.; Carpenter, J. E.; Bohmann, J. A.; Morales, C. M.; Weinhold, F. NBO 5.G; University of Wisconsin: Madison, WI, 2004.
(54) Schmidt, M. W.; Baldridge, K. K.; Boatz, J. A.; Elbert, S. T.; Gordon, M. S.; Jensen, J. H.; Koseki, S.; Matsunaga, N.; Nguyen, K. A.; Su, S. J. et al. Gamess, version 11; Iowa State University: Ames, IA, 2008.
(55) Bulat, F.; Toro-Labbé, A.; Brinck, T.; Murray, J.; Politzer, P. Quantitative Analysis of Molecular Surfaces: Areas, Volumes, Electrostatic Potentials and Average Local Ionization Energies. *J. Mol. Model.* **2010**, *16*, 1679−1693.
(56) Ditchfield, R. Self-Consistent Perturbation Theory of Diamagnetism I. A Gauge-Invariant LCAO Method for NMR Chemical Shifts. *Mol. Phys.* **1974**, *27*, 789−807.
(57) Perera, S. A.; Nooijen, M.; Bartlett, R. J. Electron Correlation Effects on the Theoretical Calculation of Nuclear Magnetic Resonance Spin−Spin Coupling Constants. *J. Chem. Phys.* **1996**, *104*, 3290−3305.
(58) Perera, S. A.; Sekino, H.; Bartlett, R. J. Coupled−Cluster Calculations of Indirect Nuclear Coupling Constants: The Importance of Non−Fermi Contact Contributions. *J. Chem. Phys.* **1994**, *101*, 2186−2196.
(59) Schäfer, A.; Horn, H.; Ahlrichs, R. Fully Optimized Contracted Gaussian Basis Sets for Atoms Li to Kr. *J. Chem. Phys.* **1992**, *97*, 2571−2577.
(60) Stanton, J. F.; Gauss, J.; Watts, J. D.; Nooijen, M.; Oliphant, N.; Perera, S. A.; Szalay, P. S.; Lauderdale, W. J.; Gwaltney, S. R.; Beck, S. et al. ACES II; University of Florida: Gainesville, FL.
(61) Murray, J.; Lane, P.; Politzer, P. Expansion of the σ-Hole Concept. *J. Mol. Model.* **2009**, *15*, 723−729.
(62) Alkorta, I.; Barrios, L.; Rozas, I.; Elguero, J. Comparison of Models to Correlate Electron Density at the Bond Critical Point and Bond Distance. *THEOCHEM* **2000**, *496*, 131−137.
(63) Alkorta, I.; Elguero, J. Fluorine-Fluorine Interactions: A NMR and AIM Analysis. *Struct. Chem.* **2004**, *15*, 117−120.
(64) Tang, T. H.; Deretey, E.; Knak Jensen, S. J.; Csizmadia, I. G. Hydrogen Bonds: Relation Between Lengths and Electron Densities at Bond Critical Points. *Eur. Phys. J. D* **2006**, *37*, 217−222.
(65) Vener, M. V.; Manaev, A. V.; Egorova, A. N.; Tsirelson, V. G. Qtaim Study of Strong H-Bonds with the O−H···A Fragment (A = O, N) in Three-Dimensional Periodical Crystals. *J. Phys. Chem. A* **2007**, *111*, 1155−1162.
(66) Palusiak, M.; Grabowski, S. J. Do Intramolecular Halogen Bonds Exist? Ab initio Calculations and Crystal Structures' Evidences. *Struct. Chem.* **2008**, *19*, 5−11.
(67) Mata, I.; Alkorta, I.; Molins, E.; Espinosa, E. Universal Features of the Electron Density Distribution in Hydrogen-Bonding Regions: A Comprehensive Study Involving H···X (X = H, C, N, O, F, S, Cl, π) Interactions. *Chem.—Eur. J.* **2010**, *16*, 2442−2452.
(68) Zeng, Y.; Li, X.; Zhang, X.; Zheng, S.; Meng, L. Insight into the Nature of the Interactions of Furan and Thiophene with Hydrogen Halides and Lithium Halides: Ab Initio and QTAIM Studies. *J. Mol. Model.* **2011**, *17*, 2907−2918.
(69) Zhang, X.; Zeng, Y.; Li, X.; Meng, L.; Zheng, S. A Computational Study on the Nature of the Halogen Bond Between Sulfides and Dihalogen Molecules. *Struct. Chem.* **2011**, *22*, 567−576.
(70) Jablonski, M.; Palusiak, M. Nature of a Hydride−Halogen Bond. A SAPT-, QTAIM-, and NBO-Based Study. *J. Phys. Chem. A* **2012**, *116*, 2322−2332.
(71) Sanchez-Sanz, G.; Trujillo, C.; Alkorta, I.; Elguero, J. Intermolecular Weak Interactions in HTeXH Dimers (X = O, S, Se, Te): Hydrogen Bonds, Chalcogen−Chalcogen Contacts and Chiral Discrimination. *ChemPhysChem.* **2012**, *13*, 496−503.